

## Physics of Extreme States of Matter — 2013

Edited by academician Fortov V.E., Karamursov B.S., Efremov V.P., Khishenko K.V.,  
 Sultanov V.G., Levashov P.R., Andreev N.E., Kanel G.I., Iosilevsky I.L., Milyavskiy V.V.,  
 Mintsev V.B., Petrov O.F., Savintsev A.P., Shapatakovskaya G.V.

ISSN 978-5-94691-533-5

Joint Institute for High Temperatures of the Russian academy of Sciences, Moscow, 2013

### CHAPTER 2. SHOCK WAVES. DETONATION. COMBUSTION

#### ELASTIC-PLASTIC PHENOMENA IN SHOCK WAVES CAUSED BY SHORT LASER PULSES. COMPARISON OF HYDRODYNAMIC AND MOLECULAR DYNAMICS SIMULATIONS

*Khokhlov V. A.<sup>1\*</sup>, Inogamov N. A.<sup>1</sup>, Zhakhovsky V. V.<sup>2</sup>, Anisimov S. I.<sup>1</sup>*

<sup>1</sup>*ITP RAS, Chernogolovka, <sup>2</sup>USF, Tampa, United States*

\*V A Kh@mail.ru

A comparison of the hydrodynamic calculations of shock waves in the target, caused by short laser pulses, using a standard equation of state and with the additional consideration of elastic shear stresses in the solid was studied.

We have included the allowance for the contribution of the elastic shear stress in the scheme of two-temperature thermo-hydrodynamic calculations.

The calculations are compared with similar calculations without elastic shear and the results of the molecular dynamics simulations and experiments reported at Elbrus-2010. This comparison shows the fundamental importance of the elastic shear stress.

*Keywords:* Hydrodynamic calculations, shock waves, shear stresses

**Introduction.** The basic difference of the solid state from other phase states is form preservation. For any deformation except isotropic compressibility there arise a shear stresses. In particular at uniaxial motion, this leads to an increase in effective rigidity and increase the velocity of deformation. In experiments on the propagation of shock waves caused by a short laser pulse, ([1–3], etc.), it was noted that these waves travel at exactly this “elastic” velocity. This is confirmed by comparison with molecular dynamics calculations ([4–6], etc.). Hydrodynamic calculations is much less resource intensive than molecular dynamics, and make it easy to include the consideration of the different effects that can directly trace their role. In particular it is possible to follow the dynamics from the significantly two-temperature stages of the laser radiation absorption by the electronic subsystem and subsequent electron-ion relaxation to the exit of the wave at the rear surface of the target in a single two-temperature thermo-hydrodynamic calculation.

**Statement of a problem and the basic equations.** In 2010, we presented the results of thermo-hydrodynamic calculations [7], simulating experiments [1, 8]. In these experiments, the laser pulse with duration of 150 fs and the energy density in the cen-

tral region of 1.3 J/cm<sup>2</sup> channeled through the glass substrate on the deposited aluminum film with thicknesses 350, 500, 760 and 1200 nm. Taking into account reflexion, the absorbed energy  $F_{abs} \approx 130$  mJ/cm<sup>2</sup>. In the calculations of the time profile of the pulse was taken Gaussian with  $\tau = 100$  fs. We used a one-dimensional Lagrangian two-temperature thermo-hydrodynamic scheme:

$$\frac{\partial x(x_0, t)}{\partial t} = v, \quad \frac{\partial x(x_0, t)}{\partial x_0} = \frac{\rho_0}{\rho}, \quad (1)$$

$$\rho_0 \frac{\partial v}{\partial x_0} = -\frac{\partial P}{\partial x_0}, \quad P = P_i(\rho, T_i) + P_e(\rho, T_e), \quad (2)$$

$$\rho_0 \frac{\partial E_e}{\partial t} = \frac{\partial}{\partial x_0} \left( \frac{\rho \kappa_e}{\rho_0} \frac{\partial T_e}{\partial x_0} \right) - P_e \frac{\partial v}{\partial x_0} - \alpha(T_e - T_i) + Q(x_0, t), \quad (3)$$

$$\rho_0 \frac{\partial E_i}{\partial t} = \frac{\partial}{\partial x_0} \left( \frac{\rho \kappa_i}{\rho_0} \frac{\partial T_i}{\partial x_0} \right) - P_i \frac{\partial v}{\partial x_0} + \alpha(T_e - T_i), \quad (4)$$

where as the Lagrangian coordinate uses coordinates  $x$  at the initial time  $x_0 = x(t = 0)$ , the density  $\rho$  at the initial time  $\rho_0 = \rho(t = 0)$  is assumed constant, the partial ionic pressure  $P_i$  and unit (per 1 mass) internal energy  $E_i$  are taken from the equation of state

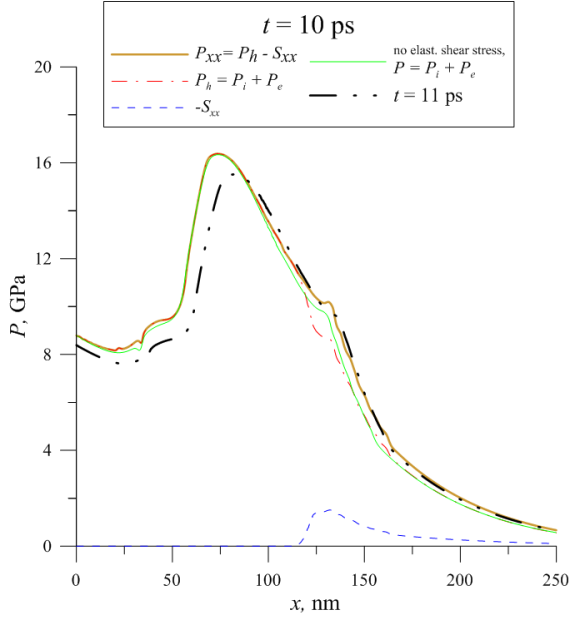


**Figure 1.** Pressure profiles at time = 10 ps. Here and below, bold line - the total pressure  $P_{xx}$ , taking into account the shear stress, dot-dash - hydrostatic pressure  $P_h$ , strokes - the shear stress  $-S_{xx}$ , thin line - pressure in the calculation without shear stress, and a thick dot-dash - the pressure beyond.

(EOS) of aluminum [9], and for electronic pressure  $P_e$  and energy  $E_e$  uses a simple analytical approximation. While EOS describes the substance at an isotropic volume compression. At uniaxial strain in the solid there is an additional shear stress, which was not taken into account in the calculation [7], and will be considered below.

In the approximation of an isotropic medium the elastic shear stress at uniaxial shear along the  $x$  axis in the linear approximation can be written as

$$S_{xx} = \frac{4}{3} G \frac{\partial(x - x_0)}{\partial x_0}. \quad (5)$$

This stress is added to the hydrostatic stress (subtracted from the pressure), making it anisotropic. Taking into account the shear stress, equation 2 becomes

$$\rho_0 \frac{\partial v}{\partial x_0} = -\frac{\partial P_{xx}}{\partial x_0},$$

$$P_{xx} = P_h - S_{xx}, \quad P_h = P_i(\rho, T_i) + P_e(\rho, T_e), \quad (6)$$

Simultaneously with the shear stress occurs the related addition to energy. Under the above assumptions contribution to the specific energy associated with the elastic shear

$$E_S = \frac{4}{3} \frac{G}{2\rho_0} \left( \frac{\partial(x - x_0)}{\partial x_0} \right)^2 \quad (7)$$

It is easy to estimate, that this contribution is small, however, near to fusion border, at temperature definition on the EOS  $T = T(\rho, E_h)$  difference  $E_h = E - E_S$

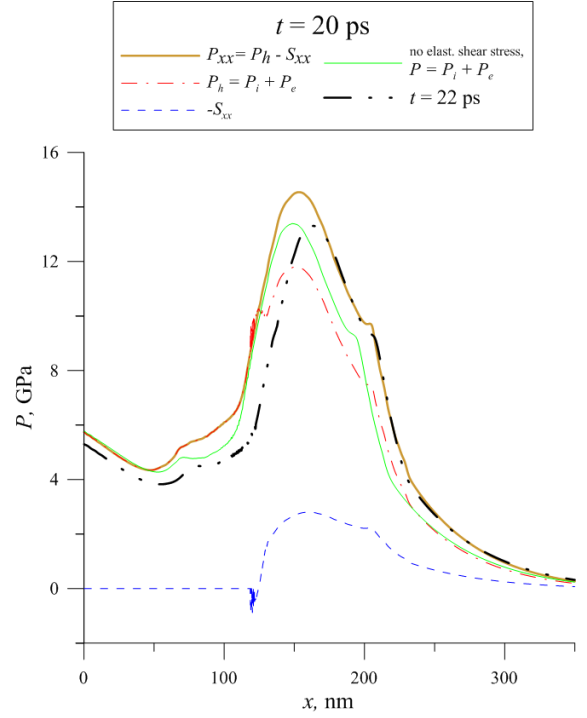


**Figure 2.** Pressure profiles at time  $t = 20$  ps

can lead to incorrect definition of a phase state of a substance.

Since

$$\rho_0 \frac{\partial E_S}{\partial t} = \frac{4}{3} G \frac{\partial(x - x_0)}{\partial x_0} \frac{\partial^2(x - x_0)}{\partial t \partial x_0} = S_{xx} \frac{\partial v}{\partial x_0}$$

in the heat balance equation the contribution of the stress energy and of the shear stress identically reduced. This is true for any balanced input, independent of temperature. Thus, the equations 3, 4 completely remain and at the account of elastic shift in the elastic solid.

In the liquid phase and more high-temperature phases shear stress is absent. Molecular dynamics simulations show that at the melting material shear stress does not disappear immediately, but at least close to the solidus, decreases gradually. For a two-phase liquid - solid region is used the following simple smoothing approximation, generalizing 5:

$$S_{xx} = F_{sol} * S_1, \quad S_1 = \frac{4}{3} G \left( \frac{\partial x}{\partial x_0} - R_c \right), \quad (8)$$

where  $F_{sol}$  - fraction of the solid phase, and  $R_c$  at first it is equal 1, and then is taken such that  $S_{xx}$  and  $S_1$  did not increase on absolute size. Accordingly the formula for energy varies also

$$E_S = \frac{1}{2\rho_0} S_{xx} \left( \frac{\partial x}{\partial x_0} - R_c \right). \quad (9)$$

Since  $F_{sol}$  depends on the  $T_i$  in the equation 4 in two-phase region it is necessary to consider directly the contribution  $E_S$  in energy and  $-S_{xx}$  in pressure. At calculations this leads to the fact that during the melting of the substance the elastic shift energy is converted

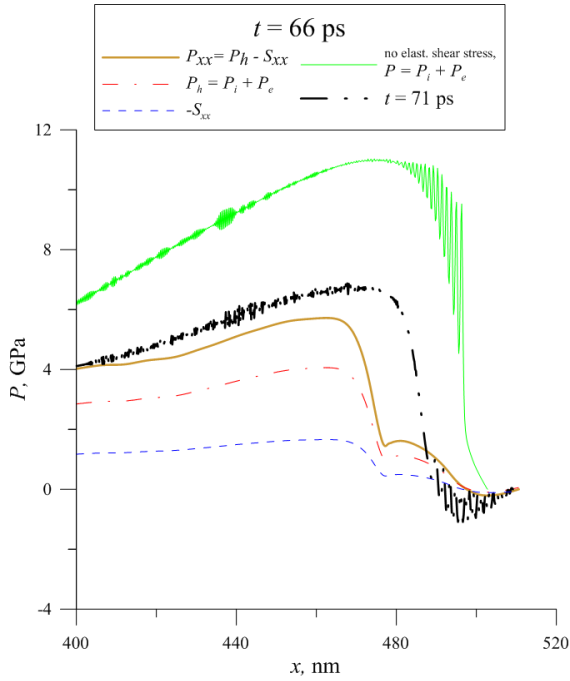


**Figure 3.** Wave exit on surface of 500 nm film ( $t = 66$  ps)

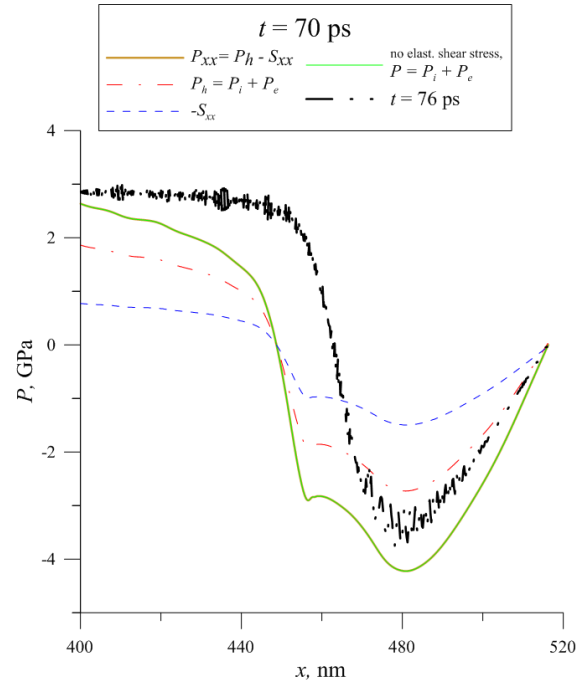


**Figure 4.** Wave after reflection of surface of 500 nm film ( $t = 70$  ps)

into thermal, increasing melting. As a result stratification of two phase area occurs faster. Comparison with molecular dynamics simulation shows that this effect exists and in the used scheme is considered insufficiently.

In the solid phase also will be used formulas 8, 9, with  $F_{sol} = 1$ ,  $R_c$  initially is 1 and at solidification after melting retains value which was at the time of solidification. In this case unphysical jump of a shear stress at solidification is absent.

**Results and discussion.** At small times, the account of elastic shear stress leads in a significant extent to the substitution of their ion pressure, total pressure varies less (see Fig. 1). The increase in the speed of the wave is visible at once. So in Fig. 1 pressure profile with the shear stress at the time  $t = 10$  ps corresponds better time  $t = 11$  ps in the calculation without shear stress. Over time, the difference becomes larger (Fig. 2).

Even more considerably distinctions are shown at a wave exit on a film surface, and, especially, after its reflexion from a surface (Fig. 3), and, especially, after its reflexion from the surface (fig. 4). Shear stress leads to a significant increase in the braking tension and hence a more rapid deceleration of the film surface.

Then, in the region of greatest tension takes place cold melting of the substance, leading to its expansion and discharge of the shear stress (Fig 5). This leads to reduced braking stress and some acceleration of of the film surface, preceding her separation. Perhaps with this mechanism is associated complex nonmonotonic motion of the film, which is observed experimentally.

A comparison of the time dependences of the shift of the film surface in the calculation with the shear stress and without it is shown in Fig. 6. It can be seen

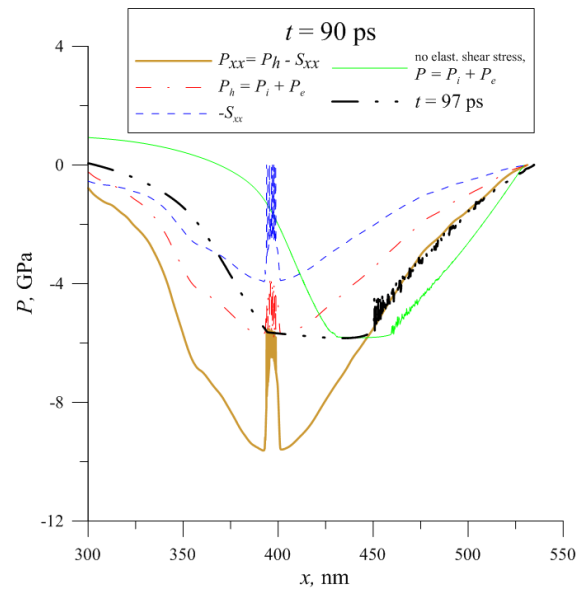


**Figure 5.** Pressure profiles at time  $t = 90$  ps

that the inclusion of shear stress leads to a much better agreement between calculations and experimental results.

**Conclusions** The calculations show the fundamental importance of shear stress in the solid in the calculations of waves induced by short laser pulses. The proposed model simulates adequately the experimental results.

This work was supported by the RAS Presidium program “Matter at high energy densities” and RFBR.

1. S.I. Ashitkov, M.B. Agranat, G.I. Kanel', *et al.* // JETP Letters. V. 92 P.516. 2010.

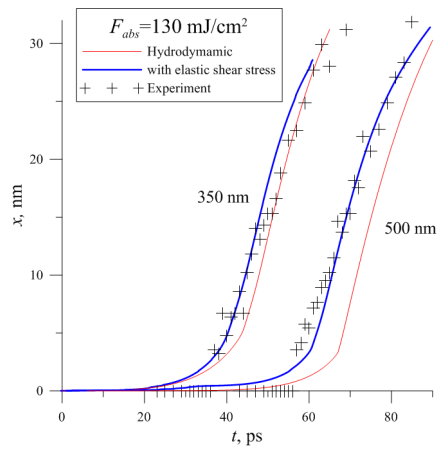


**Figure 6.** Time profiles of surface shift of 350 nm and 500 nm films

2. Armstrong, M. R., Crowhurst, J. C., Bastea, S., and Zaug, J. M., *J. Appl. Phys.* V. 108. P. 023511 (9 p.) 2010.
3. Whitley, V. H., McGrane, S. D., Eakins, D. E., *et al.* *J. Appl. Phys.* V. 109. P. 013505 (4 p.) 2011.
4. V.V. Zhakhovskii and N.A. Inogamov. *JETP Letters*, V. 92. P. 521. 2010.
5. N.A. Inogamov, V.A. Khokhlov, Yu.V. Petrov, *et al.* *AIP Conference Proceedings*. V. 1426. P. 909–912. 2012.
6. B.J. Demaske, V.V. Zhakhovsky, N.A. Inogamov, *et al.* *AIP Conference Proceedings*. V. 1426. P. 1163–1166. 2012.
7. V.A. Khokhlov, N.A. Inogamov, S.I. Anisimov, *et al.* // *Physics of Extreme States of Matter—2010* / Ed. by Fortov V. E. *et al.* Chernogolovka: IPCP RAS, 2010. P. 127–129
8. Komarov P. S., Ashitkov S. I., Ovchinnikov A. V. // *XXV Int. Conf. on Equations of State for Matter*, Book of Abstracts, Chernogolovka: IPCP RAS, 2010.
9. <http://teos.ficp.ac.ru/rusbank/>.